Cross Sections for Some N_2^+ and NII Emissions Excited by 1- to 10-keV N_2^+ on N_2

JOHN P. DOERING

University of California, Los Alamos Scientific Laboratory, Los Alamos, New Mexico

(Received 28 October 1963)

Emission cross sections for the (0,0), (0,1), and (1,2) N_2^+ first negative bands and the NII $3p\ ^3D-3d\ ^3F^0$ lines have been measured in the excitation of N_2 by a beam of 1- to 10-keV N_2^+. Light produced along a 15-cm path was integrated and analyzed with a monochromator. A 180-eV electron beam was used for calibration with the aid of the known electron $+N_2$ cross section for N_2^+ (0,0) first negative band excitation. The light output per incident particle was measured as a function of N_2 gas pressure from 0.1 to 20 microns at each energy. Cross sections were calculated on the basis of a mechanism which predicted the observed pressure variation of light output. The N_2^+ first negative system emission cross sections were found to reach a broad maximum near 7 keV while that for NII increased throughout the energy range studied. Doppler shift experiments showed that most of the N_2^+ emission observed was the result of charge exchange processes. The NII emissions appear to be excited by violent ionizing collisions. The maximum value of the N_2^+ first negative band (0,0) emission cross section was found to be 1.2×10^{-17} cm^2.

I. INTRODUCTION

WHEN molecular ions, such as N_2^+, are incident on their own gas, a variety of charge transfer processes can take place. The most extensively investigated of these is exact resonance charge exchange in which the ion and molecule remain in their ground electronic states. There is also, however, the possibility that one or both of the products of the charge exchange encounter may be left in excited electronic states from which optical emission can be observed. Vibrational and rotational excitation are also possible. Since the relation of the cross sections for production of various excited states to the exact resonance charge exchange cross section is of considerable importance to the basic understanding of the nature of the charge exchange process, it was felt to be desirable to make a detailed study of cross sections for excitation of molecular and atomic spectral features in a system in which exact resonance charge exchange was possible. Although nitrogen may appear to be a poor choice for such an investigation due to its theoretical complexity, its predominant role in atmospheric processes gives such data considerable practical importance.

Previous investigations[1-4] of optical excitation by ion bombardment of nitrogen in the energy region less than 50 keV have been mainly centered around the system H^++N_2 which is of direct auroral significance. Carleton and Neff[5] have also measured emission cross sections for a number of different bands in the bombardment of N_2 by various ions, including N_2^+, in the 400–3000-eV range.

One of the problems most frequently encountered by previous investigators has been the discrimination against excitation by fast neutral particles produced by charge exchange. In the present experiment, light pro-

duced by both primary ions and fast neutrals along an extended path has been combined by the use of a light integrating device. If the mechanism of excitation is well established and the total charge exchange and neutral-neutral ionization cross sections for the system are known, it is possible to extract the excitation cross sections for ionic and neutral impact from the dependence of light output on the pressure of neutral gas. The method used in this case will be described in detail below.

For such an approach to be valid, however, the optical excitation processes considered must have relatively simple mechanisms. Otherwise, the integral over many primary and secondary processes is so complex that recovery of cross section data is impossible. In practice, this means that emission cross sections for the N_2^+ first negative bands and NII lines, which appear to be excited solely by primary beam particle impact, can be obtained; but the N_2 positive systems, which can be excited by any primary or secondary particle cannot be successfully studied.

II. EXPERIMENTAL METHOD

General

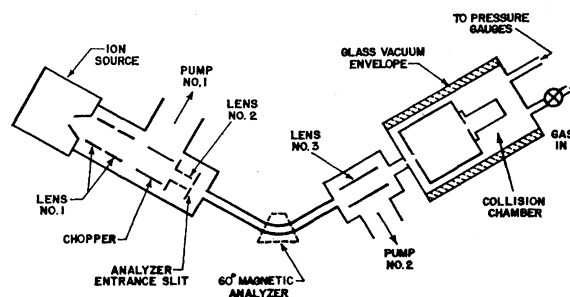A schematic diagram of the apparatus is shown in Fig. 1. Ions were formed in a conventional Duoplasma-

[1] C. Y. Fan, Phys. Rev. **103**, 1740 (1956).

[2] N. P. Carleton, Phys. Rev. **107**, 110 (1957).

[3] N. P. Carleton and T. R. Lawrence, Phys. Rev. **109**, 1159 (1958).

[4] W. F. Sheridan, O. Oldenberg, and N. P. Carleton, *Second International Conference on the Physics of Electronic and Atomic Collisions (Abstracts)* (W. A. Benjamin, Inc., New York, 1961).

[5] S. H. Neff, thesis, Harvard University, 1963 (unpublished).

FIG. 1. Schematic diagram of the apparatus.

tron ion source[6] and focused into a beam with an einzel lens system. The beam was passed through a parallel plate electrostatic deflection type chopper which interrupted it at a 30-cps rate. After leaving the chopper, it was refocused with a second lens and entered a conventional 60° magnetic analyzer. From the mass analyzer, the beam was focused onto the entrance aperture of the collision chamber with a third lens. N_2^+ currents ranged from 0.1 to 5 μA.

The ion source region was evacuated with a liquid nitrogen-trapped oil diffusion pump having an effective speed at the source region of 500 liters/sec. The region between the mass analyzer and collision chamber was evacuated with a 400 liters/sec Vacion pump which kept the pressure in this region below 5×10^{-5} mm with collision chamber pressures up to 20 μ.

Collision chamber pressure was measured with a liquid nitrogen-trapped McLeod gauge or Pirani and ion gauges which had been calibrated against the McLeod gauge.

"Water pumped" nitrogen (99.7% pure, O_2 0.3% max) was used without further purification for both ion source and collision chamber. No emissions from other than atomic and molecular nitrogen and their ions were observed when the collision chamber gas was in contact with the McLeod gauge cold trap. Without this trap, Balmer emissions appeared in the spectra, presumably from traces of water vapor.

Collision Chamber

A detailed schematic diagram of the collision chamber is shown in Fig. 2. The vacuum envelope was a 6-in.-
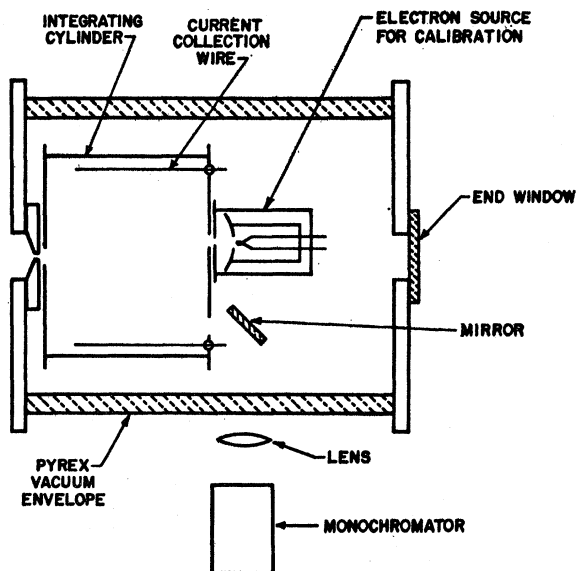

FIG. 2. Schematic diagram of collision chamber with light integrating cylinder in place.

[6] C. D. Moak, H. E. Banta, J. N. Thurston, J. W. Johnson, and R. F. King, Rev. Sci. Instr. **30**, 694 (1959).

diam Pyrex tee through which the light passed to the spectroscopic apparatus. For the measurements in which it was desired to integrate the light produced by the beam along its path, a brass cylinder 12.5 cm in diameter and 15.2 cm long was placed inside the vacuum envelope. The ion beam entered this cylinder through an opening on the axis. The inside of the cylinder was smoked with a heavy layer of magnesium oxide to provide diffuse reflectance. A hole off the axis with a mirror allowed light from a path parallel to the beam to be focused on the slit of the monochromator with an achromatic lens.

Difficulty was anticipated in the measurement of current to the integrating cylinder since the inner surface of this device was coated with a good insulator. For this reason, two bare copper wires, insulated from the cylinder, were inserted into it parallel to its axis. One of the wires was electrically connected to the cylinder and a battery was connected between this combination and the other wire. It was hoped that the application of a weak field between the wires would aid in the collection of secondary particles. Tests with various battery voltages, however, produced no significant change in the total positive ion current from the cylinder to ground. The battery was therefore eliminated and the cylinder and the two wires connected electrically and used as the collector. Apparently, surface charge on the insulating coating helped in the collection of secondary particles on the copper wires.

For the higher resolution spectroscopy and Doppler experiments, the integrating cylinder assembly was removed from the collision chamber. The beam traversed a 41-cm path before hitting the end window and flange. The light produced was viewed through the end window to observe Doppler shift.

Calibration Method

The excitation of N_2 by electrons of a few hundred volts energy provides a means for calibration of an apparatus such as this one. The cross section for electron excitation of the N_2^+ (0,0) first negative band ($\lambda 3914$ Å) has been measured by at least two different sets of investigators[4,7] with good agreement in results.

A small electron source was mounted on the end of the integrating cylinder opposite the ion beam entrance and slightly off the axis of the cylinder (Fig. 2). The integrated light output from the 15-cm path was linear with current and linear with pressure up to pressures of one μ. Above this pressure the light output began to fall off slightly.

Calibration was performed with 180-eV electrons pulsed at a 30-cps rate. N_2 pressures used were 0.1 to 1.0 μ. From a knowledge of the electron current, path length, gas density, and cross section for N_2^+ (0,0) first negative excitation (taken to be 5.3×10^{-18} cm^2 at 180 eV) the number of photons emitted along the

[7] D. T. Stewart, Proc. Phys. Soc. (London) **69**, 437 (1956).

path was calculated and the apparatus was calibrated without geometrical difficulties.

The calibration described above was performed frequently to calibrate the apparatus at a wavelength of 3914 Å. In order to determine the response at other wavelengths, a calibrated tungsten ribbon filament lamp was used. The mirror shown in Fig. 2 was eliminated and the image of the lamp filament instead of the image of the opening in the integrating cylinder was focused onto the monochromator slit. A filter of known transmission which blocked radiation above 4000 Å was used to show that scattered light inside the monochromator was not a significant problem except at wavelengths less than 3400 Å. The relative response of the detection system was thus determined for the region of interest in this experiment which was 3900 to 5000 Å.

Spectroscopic Apparatus

The basic instrument used for the cross section measurements was a 0.5-m Bausch and Lomb grating monochromator. The main problem arising with this instrument was the choice of a suitable slit width. The instrument had a dispersion of 36 Å/mm and so a slit width of 0.75 mm was used in the hope that this would provide maximum intensity by including the entire band, while providing maximum discrimination against unwanted spectral features. The instrument wavelength setting was adjusted for maximum signal from each spectral feature to be examined. The severe aberrations in this instrument made it useless for measurement of vibrational band contours.

For higher resolution spectral work, a 0.5-m scanning Jarrell Ash Company monochromator was used. The grating in this instrument was blazed for near 7000 Å in the first order so all the spectral features from 3300 to 5500 Å were observed in the second order for maximum intensity and dispersion. This instrument proved capable of resolving the N_2^+ first negative (0,0) band rotational structure.

The detection apparatus was an EMI photomultiplier which was run at 1000 V. The ac signal from the chopped light source (either the ion or electron beam) was amplified in a selective 30-cps low-noise preamplifier and detected with a Princeton Applied Research Corporation lock-in amplifier.

Survey spectra were also taken with an $f\,0.9$ auroral spectrograph using 103 aF film. This instrument had a first-order dispersion of 200 Å/mm. It had few advantages over the photoelectric scanning monochromator and so was not extensively used.

III. RESULTS

Results of Survey Spectra

The first spectra of this source were taken using the $f/0.9$ auroral spectrograph. In a wavelength region 3800–6800 Å, the N_2^+ first negative system, N_2 first

and second positive system, and some N_{II} lines were observed.

More recent spectra, taken photoelectrically with the 0.5-m Jarrel Ash Company scanning monochromator, show the same features, except for the first positive system in a wavelength region 3300–5500 Å.

In neither case was it possible to identify N_I emissions although N_{II} was an extremely prominent part of the spectrum. The strongest observed N_{II} lines arose from the following transitions: $3d\ ^1F^0\text{–}4f\ ^1G$, $3D\ ^3F^0\text{–}4f\ ^3G$, $3p\ ^3D\text{–}3d\ ^3F^0$, $3s\ ^1P^0\text{–}3p\ ^1D$, $3s\ ^3P^0\text{–}3p\ ^3D$, $3s\ ^1P^0\text{–}3p\ ^1P$.[8] N_2^+ first negative bands were observed up to the (3,5) transition and N_2 second positive (3,5) was also observed.

High resolution spectra of the N_2^+ (0,0) first negative band were also taken. An example is shown in Fig. 3. A calculation of the rotational temperature gives $T_{\rm rot}=475°K$. The fact that N_2^+ impact produces an excited rotational distribution is interesting in that proton impact has been found to produce rotational temperatures equal to the gas temperature. The longer collision time in the case of N_2^+ impact may be responsible for the effect here which is similar to that observed in the bombardment of N_2 by 1- to 3-keV Li^+ ions.[9]
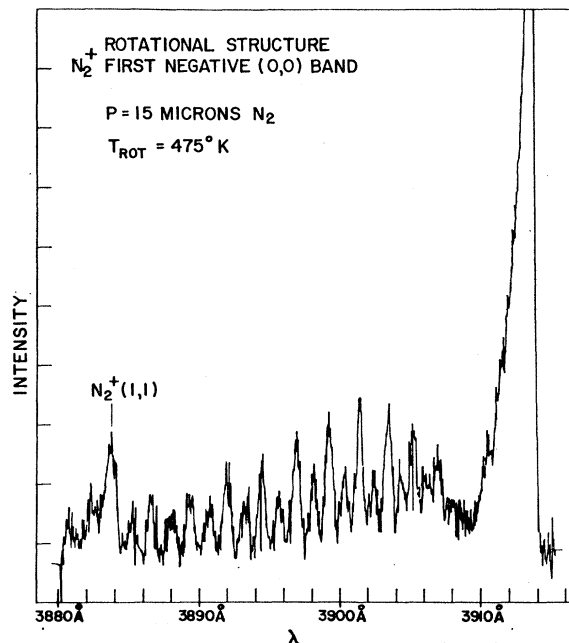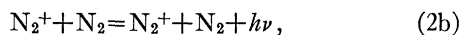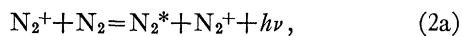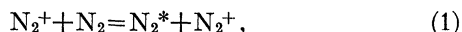

FIG. 3. N_2^+ (0,0) first negative band ($\lambda3914$ Å) excited by 10-keV N_2^+ on N_2. The rotational temperature calculated from this spectrum is 475°K.

[8] C. E. Moore, *A Multiplet Table of Astrophysical Interest* (Princeton University Observatory, Princeton, New Jersey, 1945).
[9] E. M. Reeves and R. W. Nicholls, Proc. Phys. Soc. (London) 78, 588 (1961).

Mechanism of N_2^+ Optical Excitation

In order to observe optical emission in the first negative system of N_2^+ when N_2 is bombarded by N_2^+, we must either produce an N_2^+ ion and excite it to the $B\ ^2\Sigma_u^+$ state or excite an existing N_2^+ ion. The processes which may lead to such excitation are

$$N_2^+ + N_2 = N_2^* + N_2^+, \tag{1}$$

$$N_2^+ + N_2 = N_2^* + N_2^+ + h\nu, \tag{2a}$$

$$N_2^+ + N_2 = N_2^+ + N_2 + h\nu, \tag{2b}$$

$$N_2^* + N_2 = N_2^+ + e + N_2, \tag{3}$$

$$N_2^* + N_2 = N_2^+ + e + N_2 + h\nu. \tag{4}$$

(1) includes all charge exchange events which do not lead to optical emission at the wavelength in question. (2a) is charge exchange with production of an N_2^+ first-negative photon. It is possible that the electron will not be captured in a few of (1) and (2a) events. (2b) is collisional excitation of the beam particles with photon production. (3) includes neutral-neutral ionization events which arise from collisions between fast neutrals (N_2^*) produced in (1) and the background gas. Either the fast beam particle or the thermal gas molecule may lose an electron to produce N_2^+. (4) is ionization by fast neutral impact accompanied by N_2^+ first negative system emission. As in (3), either a fast beam particle or a thermal gas molecule may be ionized and excited. If we take (2a) and (2b) together for the moment and designate the total cross section for the two processes σ_2, we have for the number of photons radiated from an increment of path dl per unit time:

$$dI/dl = \sigma_2 f(N_2^+)N + \sigma_4 f(N_2^*)N. \tag{5}$$

$f(N_2^+)$ and $f(N_2^*)$ are the number of primary ions and fast neutral particles which cross a plane perpendicular to the beam per unit time after the beam has traversed a path of arbitrary length through the gas. We have taken N to be the total N_2 gas density.

The apparatus, however, integrates light produced at all points along the path in the integrating cylinder. We must, therefore, integrate I along l. This requires a knowledge of the number of charged and uncharged particles incident on the increments of path length per unit time. Since the radiative reactions (2) and (4) will have cross sections much smaller than those for the total charge exchange (1) and neutral-neutral ionization (3) processes, we can say that the dependence of $f(N_2^+)$ on l is given by

$$d[f(N_2^+)]/dl = -\sigma_1 f(N_2^+)N + (\sigma_3/2)f(N_2^*)N, \tag{6}$$

where we have assumed that the cross section for electron loss by the fast neutral particle in (3) is one-half the total cross section. Neglecting the probably small part of the beam which will be dissociated into N and N^+ by charge exchange and ionization, we have, from conservation of the beam particles,

$$i_0 = f(N_2^+) + f(N_2^*), \tag{7}$$

where i_0 is the total number of N_2^+ beam particles entering the collision chamber per unit time. Integrating (6) with the aid of (7) and (5) with the aid of the integrated form of (6), we have

$$I/i_0 = \left[\frac{\sigma_2\sigma_3/2 + \sigma_1\sigma_4}{\sigma_1 + \sigma_3/2}\right]Nx + \frac{\sigma_1(\sigma_2 - \sigma_4)}{(\sigma_1 + \sigma_3/2)^2}$$
$$\times \{1 - \exp[-(\sigma_1 + \sigma_3/2)Nx]\}, \tag{8}$$

where x is the total path length.

(8) describes the variation of the number of photons produced per incident particle with path length and density of gas. Since x is a fixed parameter of the apparatus, we can experimentally measure I/i_0 by varying N. The shape of the curve so obtained will be determined by the relative magnitudes of the cross sections for (1) through (4).

From the value of σ_1 obtained by Stebbings, Turner, and Smith[10] we can estimate the value of N at which the exponential will become much less than unity. It is apparent that for $x=15$ cm, the exponential may be neglected above pressures of $4\ \mu$.

If the charged particles produce more light through (2) than the fast neutrals (4), a plot of I/i_0 versus N from (8) will be convex upwards below $4\ \mu$ since $\sigma_2 > \sigma_4$. If $\sigma_2 = \sigma_4$, we will have a straight line through the origin. Finally, if $\sigma_2 < \sigma_4$, the curve will be concave upwards below $4\ \mu$ and the intercept extrapolated from the high-pressure linear segment will be negative.

A typical experimental plot of I/i_0 versus pressure for N_2^+ first negative emission is shown in Fig. 4. Since the curve is convex upwards below $4\ \mu$, we can say im-
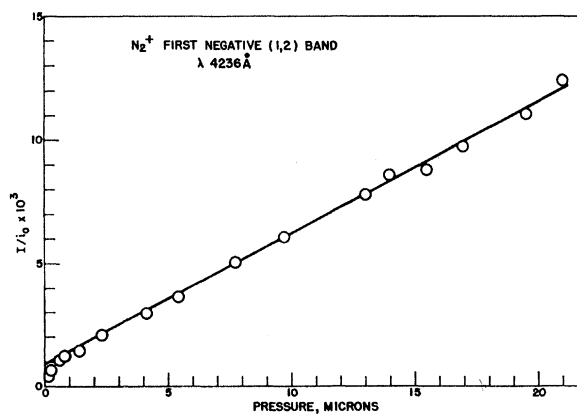

FIG. 4. Typical experimental I/i_0 versus pressure results for N_2^+ first negative system. The emission shown here is the (1,2) N_2^+ first negative band ($\lambda 4236$ Å).

[10] R. F. Stebbings, B. R. Turner, and A. C. H. Smith, J. Chem. Phys. 38, 2277 (1963).

mediately $\sigma_2 > \sigma_4$. Other measurements show I to be linear with i_0 as required by (8).

As an additional check on the validity of the proposed mechanism, we note that if (8) is written

$$I/i_0 = A\{1 - \exp[-(\sigma_1 + \tfrac{1}{2}\sigma_3)Nx]\} + BNx, \quad (9)$$

we have

$$\ln[(A + BNx) - (I/i_0)] = -(\sigma_1 + \tfrac{1}{2}\sigma_3)Nx + \ln(A). \quad (10)$$

$(\sigma_1 + \sigma_3/2)$ may be calculated from experimental data using (10). The results of such calculations have been previously reported.[11] A value for $(\sigma_1 + \sigma_3/2)$ of $(2.6 \pm 0.4) \times 10^{-15}$ cm² was obtained at an ion energy of 5500 eV. If σ_3 is of the order of 3×10^{-16} cm², then our value σ_1 is 2.4×10^{-15} cm², in satisfactory agreement with Stebbings, Turner, and Smith[10] who find $\sigma_1 = 1.95 \times 10^{-15}$ cm² at the same energy.

N₂⁺ First-Negative Emission Cross Section Results

From the experimental plots of I/i_0 versus pressure at each energy, we can measure the slope and extrapolated intercept of the high-pressure linear segment of the curve. These two experimental parameters give us σ_2 and σ_4 since

$$\sigma_2 = A(\sigma_1 + \tfrac{1}{2}\sigma_3) + B/x \quad (11)$$

$$\sigma_4 = B/x - \tfrac{1}{2}A\sigma_3[1 + (\tfrac{1}{2}\sigma_3/\sigma_1)]. \quad (12)$$

We must, however, know σ_1 and σ_3 as a function of energy to get absolute values for σ_2 and σ_4. We have used values of σ_1 from Stebbings, Turner, and Smith[10] and have extrapolated their data to 10 keV where necessary. This procedure should not introduce an important uncertainty since the energy variation of σ_1 in the range 2 to 10 keV seems to be slight.

σ_3, however, has been measured only to 800 eV.[12] In the calculation of σ_2, σ_3 can be neglected since $\sigma_3/2$ is undoubtedly much less than σ_1, and we have done so for our calculations. However, since (12) involves a difference of terms of the same order of magnitude, we must have accurate knowledge of σ_3 as a function of energy to calculate σ_4. For this reason, we have calculated only σ_2 from our data. σ_4 can be estimated at 1 keV and appears to be near 3×10^{-19} cm².

I/i_0 was measured as a function of pressure at each energy. A and B were then computed and the emission cross section determined. Results for N₂⁺ first negative (0,0) band excitation are shown in Table I. The value taken for σ_1 at each energy is included. Emission cross section results are plotted versus ion energy in Fig. 5. Also shown are the results for the (0,1) band and Carleton and Neff's results for the (0,0) band.[5] Since the

(0,0) and (0,1) transitions originate from the same upper state, the cross sections for the two should differ by the relative transition probability. Analysis of the data of Fig. 5 gives

$$\sigma_{(0,1)}/\sigma_{(0,0)} = 0.30 \pm 0.04.$$

This result is not in agreement with that of Wallace,[13] who finds a ratio of 0.42, but is in good agreement with Tyte,[14] who gives a ratio of 0.25 for intensities or 0.27 for cross sections.

The cross sections for the (0,0) and (0,1) first negative bands reach a broad maximum near 7 keV. In order to predict the position of the maximum in such cross section versus energy curves, it is customary[15] to set the quantity $a\Delta E/h\nu$ from the adiabatic criterion of Massey[16] equal to unity. The maxima in these cross section energy curves can be predicted in this way if a is taken to be of the order of 3×10^{-8} cm. This is a smaller value of a than is usually associated with such processes. Considering the extremely crude theoretical basis of this procedure, however, such agreement is all that can be expected.
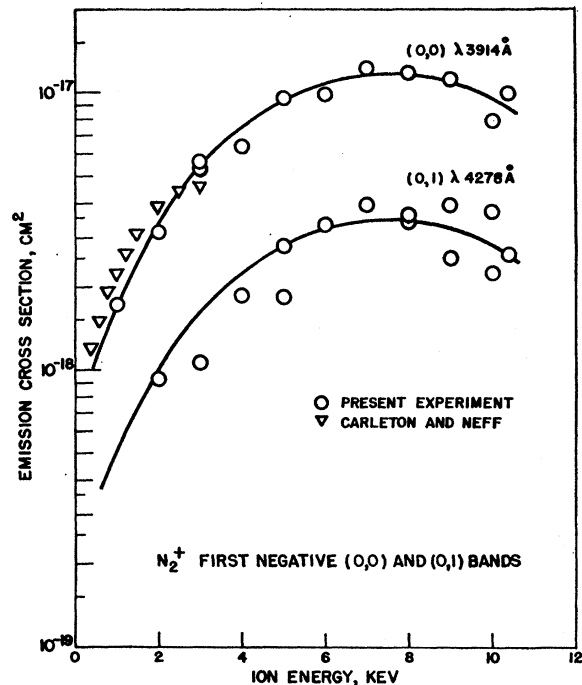

FIG. 5. Emission cross sections versus ion energy for N₂⁺ first negative (0,0) (λ3914 Å) and (0,1) (λ4278 Å) bands. The (0,0) band data of Carleton and Neff (Ref. 5) are included for comparison.

[11] J. P. Doering and R. F. Holland, Bull. Am. Phys. Soc. **8**, 299 (1963).

[12] N. G. Utterback and G. H. Miller, Phys. Rev. **124**, 1477 (1961).

[13] L. W. Wallace, thesis, University of Western Ontario, 1954 (unpublished).

[14] D. C. Tyte, Proc. Phys. Soc. (London) **80**, 1364 (1962).

[15] J. B. Hasted, Proc. Roy. Soc. (London) **A205**, 421 (1951).

[16] H. W. S. Massey and E. H. S. Burhop, *Electronic and Ionic Impact Phenomena* (Oxford University Press, New York, 1952).

TABLE I. A summary of experimental results. The value assumed for the total charge exchange cross section (σ_1) is shown as well as the value for A and B obtained from each experiment. The emission cross section was calculated from (11) taking $x=15$ cm.

Run No.	E (keV)	σ_1 (cm²)	A	B (cm³)	Emission cross section (cm²)
		N₂⁺ First-negative (0,0) band (λ 3914 Å)			
81	8.0	1.75×10^{-15}	4.1×10^{-3}	7.1×10^{-17}	11.9×10^{-18}
82	6.0	1.86	3.8	4.3	9.9
83	4.0	2.00	2.4	2.4	6.4
85	3.0	2.08	2.0	2.1	5.6
87	2.0	2.18	1.3	0.7	3.1
89	10.0	1.65	2.3	6.3	7.9
91	10.4	1.63	3.4	6.7	9.9
97	9.0	1.92	3.3	7.1	11.1
98	7.0	1.80	4.8	4.7	12.2
99	5.0	1.92	3.9	3.1	9.6
100	3.0	2.08	2.1	1.7	5.4
101	1.0	2.30	0.6	0.5	1.72
		N₂⁺ First-negative (0,1) band (λ 4278 Å)			
77	8.0	1.75×10^{-15}	12.7×10^{-4}	19.0×10^{-18}	3.5×10^{-18}
78	10.0	1.65	12.0	27.2	3.8
79	5.0	1.92	9.7	14.3	2.8
80	9.0	1.70	13.3	26.0	4.0
81	8.0	1.75	12.2	22.4	3.6
82	6.0	1.84	13.3	13.6	3.3
83	4.0	2.00	[6.8	7.7	1.9
88	2.0	2.18	3.8	1.8	0.94
89	10.0	1.65	[5.9	19.2	2.2
92	10.4	1.63	[7.9	20.0	2.6
93	9.0	1.70	[7.3	19.6	2.5
94	7.0	1.80	15.1	19.7	4.0
95	5.0	1.92	6.4	9.3	1.8
96	3.0	2.18	4.2	2.2	1.1
		N₂⁺ First-negative (1,2) band (λ 4236 Å)			
102	8.0	1.75×10^{-15}	9.7×10^{-4}	15.7×10^{-18}	27.2×10^{-19}
103	6.0	1.86	3.6	11.2	14.1
104	10.0	1.65	1.9	16.6	14.0
105	9.0	1.70	2.4	19.7	17.2
106	7.0	1.80	5.7	17.2	21.5

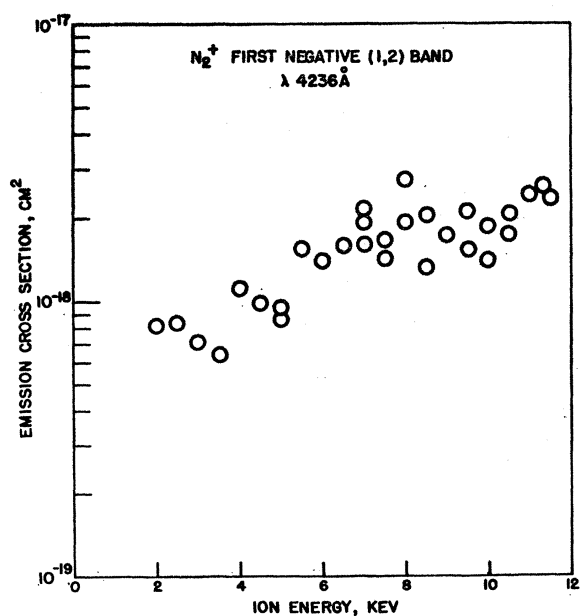| Run No.	E (keV)	σ_1 (cm²)	A	B (cm³)	Emission cross section (cm²)
		N₂⁺ First-negative (1,2) band (λ 4236 Å)			
107	11.5	1.56×10^{-15}	7.9×10^{-4}	16.7×10^{-18}	23.4×10^{-19}
108	10.5	1.62	4.0	16.5	17.3
109	8.0	1.75	6.0	13.8	19.1
110	9.5	1.67	1.6	19.2	15.2
111	11.25	1.58	7.6	21.1	25.9
112	4.0	2.00	2.7	8.7	11.2
113	2.0	2.18	2.5	4.4	8.2
114	5.0	1.92	1.2	9.6	8.6
115	8.5	1.72	1.4	16.3	13.1
116	7.0	1.80	4.6	11.7	16.0
118	5.0	1.92	1.3	10.6	9.5
119	4.5	1.96	2.3	8.2	9.9
120	8.5	1.72	3.8	21.4	20.1
121	6.5	1.83	3.8	13.6	15.9
122	5.5	1.90	4.0	11.9	15.3
123	7.5	1.80	3.8	15.1	16.8
124	10.0	1.65	4.0	18.4	18.7
125	11.0	1.60	6.9	19.9	24.1
126	10.5	1.62	3.1	24.2	20.9
127	7.5	1.78	2.3	15.2	14.1
128	7.0	1.80	5.4	14.3	19.1
129	3.0	2.08	1.2	6.7	7.0
130	9.5	1.87	3.7	21.4	21.0
131	2.5	2.14	2.5	4.5	8.3
132	3.5	2.04	0.8	7.4	6.4
		$N_{II}\ 3p\ ^3D-3d\ ^3F^0$ (λ 5005 Å)			
135	10.0	1.65×10^{-15}	17.0×10^{-5}	15.1×10^{-18}	12.7×10^{-19}
136	7.0	1.80	8.5	8.6	7.2
137	5.0	1.93	8.9	4.1	4.4
138	6.0	1.86	10.9	6.7	6.4
139	8.0	1.75	13.1	11.9	10.1
140	9.0	1.70	8.7	13.1	10.1
141	11.0	1.60	26.3	17.5	15.7
142	4.0	2.00	5.9	3.0	3.2
143	3.0	2.10	1.2	1.6	1.3

FIG. 6. Emission cross section versus ion energy for N₂⁺ first negative (1,2) band (λ4236 Å).

The cross section for (1,2) excitation is shown in Fig. 6 and the data are tabulated in Table I. This curve has the same general shape as that for (0,0) and (0,1) excitation although it does not, perhaps, drop off quite so quickly at low energies.

The transition probabilities for the (0,0), (0,1), and (0,2) N₂⁺ first negative bands are given by Wallace[13] as 0.539, 0.230, 0.070, respectively. We can conclude that the cross section for the 0 vibrational state of $N_2^+B\ ^2\Sigma_u^+$ is near 1.5×10^{-17} cm² at the maximum using the data of Fig. 5. The transition probabilities for (1,0), (1,1), (1,2), (1,3), (1,4) bands are also given by Wallace as 0.21, 0.22, 0.27, 0.26, 0.05, respectively. We therefore estimate the total 1-level cross section at the maximum to be about four times that for the (1,2) or 8×10^{-18} cm². This leads us to the conclusion that the cross section for population of the first-excited vibrational level of $N_2^+B\ ^2\Sigma_u^+$ is only a factor of two less than that for population of the ground vibrational state.

It should be noted that the scatter in the experimental data on emission cross sections, which is unfortunately large in the case of the (1,2) band, comes almost entirely from difficulty in the determination of the value of the
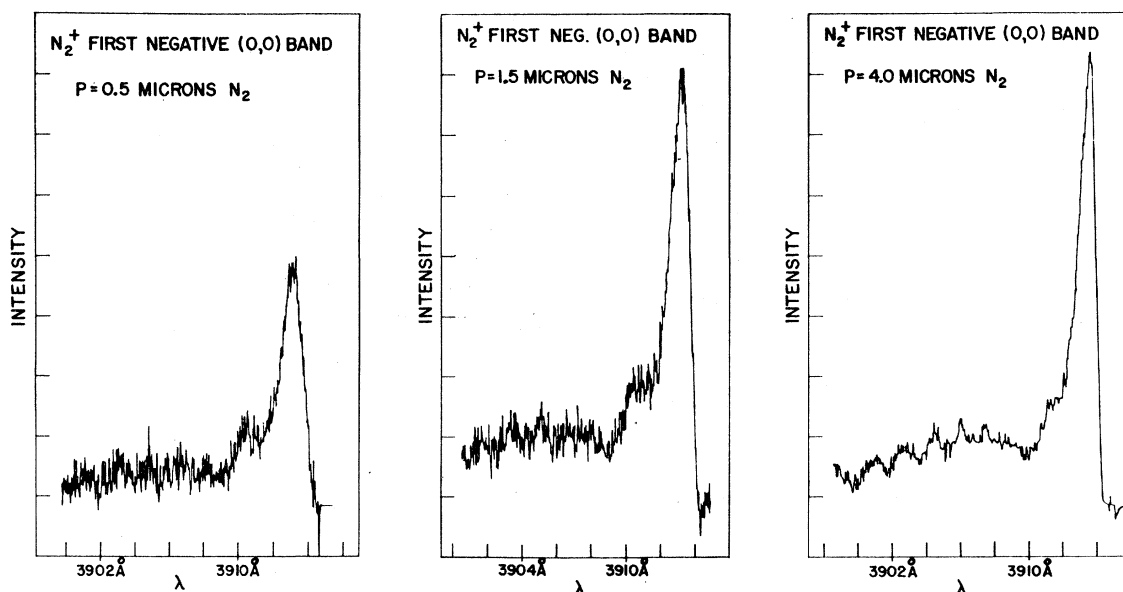
FIG. 7. Spectra of $N_2{}^+$ first negative (0,0) band ($\lambda 3914$ Å) excited by 10-keV $N_2{}^+$ on N_2 at three different pressures. The Doppler-shifted component ($\lambda 3910.4$ Å) decreases relative to the unshifted component with increasing pressure.

extrapolated intercept A. Unfortunately, the quantity $A\sigma_1$ is of the same order as B/x in the cases considered here. It is, of course, much easier to determine the slope B than the intercept A. We therefore find, from an examination of the data in Table I, that plots of B/x versus energy give smooth curves while corresponding plots of $A\sigma_1$ show extreme amounts of scatter as in the (1,2) case. This difficulty is the main weakness of this experimental method. Fortunately, in the case of the (0,0) first negative band, enough intensity is available to make an accurate determination of A possible.

$N_2{}^+$ First Negative System Doppler Results

An examination of the light emitted from ion bombardment for Doppler shift can, in principle, distinguish between excitation of the gas by charge exchange processes, which produce mainly thermal ions (2a), and excitation of the beam particles by simple collisions or ionization such as (2b) and (4).

Spectra of the $N_2{}^+$ first negative (0,0) band excited by 10-keV $N_2{}^+$ taken at three different pressures through the end window of the collision chamber are shown in Fig. 7. The Doppler-shifted component is approximately 0.2 times the unshifted component at a pressure of 0.5 and 1.5 μ, decreases to perhaps one-half this at 4 μ, and is not visible at 15 μ (Fig. 3). The mechanism (1) through (4) does not predict a change in the relative magnitudes of shifted and unshifted components except at very low pressures. This effect can, however, be explained by quenching of the shifted component through charge exchange.

The lifetime of the $v'=0$ level of the $N_2{}^+$ first negative system upper state ($B\,{}^2\Sigma_u{}^+$) has been measured by

Bennett and Dalby and is 6.6×10^{-8} sec.[17] We must compare this lifetime with the time required for an excited high-energy beam particle to charge exchange. Taking $\sigma_1 = 1.7 \times 10^{-15}$ cm^2 at[10] 10 keV we have, at 4 μ, a time between charge exchange events of 1.5×10^{-7} sec. At this pressure, therefore, 90% of the excited ions would radiate before charge exchanging. However, σ_1 may be appreciably larger than 1.7×10^{-15} cm^2 for charge exchange between $N_2{}^+B\,{}^2\Sigma_u{}^+$ and N_2. A factor of two increase in σ_1 would produce an effect of the order of magnitude observed.

This quenching process may introduce an error into the measurement of cross sections if the Doppler-shifted component of the band is lost at high pressure. Due to the relatively small magnitude of the shifted component, however, it does not seem probable that such an error would be serious when compared with the other sources of uncertainty in the cross section measurement.

Examination of the (1,1) and (1,2) $N_2{}^+$ first-negative bands failed to disclose a Doppler-shifted component. This experiment cannot, however, be regarded as conclusive for several reasons. The lowest available pressure was 10 μ due to the weak intensity of these emissions. The (1,1) and (1,2) bands also lie in the rotational structure of the stronger (0,0) and (0,1) bands. It is, therefore, only possible to say that the shifted component of these bands is of no greater importance than that of the (0,0) band.

The ratio of intensities of shifted to unshifted components of the (0,0) band was approximately 0.20 at 0.5 and 1.5 μ pressure. We also concluded previously
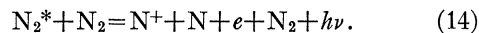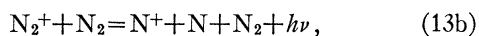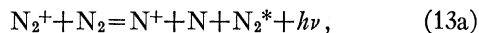
[17] R. G. Bennett and F. W. Dalby, J. Chem. Phys. 31, 434 (1959).

that σ_2 was larger than σ_4. These effects could be produced by (2a) and (2b) with or without the addition of (4). However, the data in Table I cannot be reconciled if σ_4 is taken to be zero unless σ_3 is taken to be of the order of σ_1. Since this is almost certainly not the case, we conclude that the radiation observed is produced by (2a), (2b), and (4). The collisional excitation of the beam particles (2b) probably does occur but cannot be comparable to the charge-exchange excitation (2a).

NII Emission Cross Section Results

An emission cross section was measured for those NII lines which occur near 5000 Å. Spectra of this region showed that the several lines observed could be attributed to the transition $3p\,^3D{-}3d\,^3F^0$ with associated Doppler-shifted components.

The mechanism of excitation of NII is assumed to be (1) and (3) with the addition of

$$N_2^+ + N_2 = N^+ + N + N_2^* + h\nu, \qquad (13a)$$

$$N_2^+ + N_2 = N^+ + N + N_2 + h\nu, \qquad (13b)$$

$$N_2^* + N_2 = N^+ + N + e + N_2 + h\nu. \qquad (14)$$

This mechanism is analogous to the one proposed for N_2^+ first-negative system excitation. A calculation of the expected dependence of I/i_0 on N for NII emissions leads to an expression equivalent to the one already derived for N_2^+ excitation.

A typical experimental plot of I/i_0 versus pressure for NII 5000 Å emissions is shown in Fig. 8. It must be noted that the extrapolated intercept A from these data is smaller relative to the slope B than in the N_2^+ excitation case. This shows that $\sigma_{13} > \sigma_{14}$ but the two are relatively closer in value than σ_2 and σ_4. I was also found to be linear with i_0.

Data from a study of this NII emission is shown in Table I and a plot of σ_{13} versus incident ion energy is given in Fig. 9. This cross section is seen to rise throughout the range of energy investigated. Such behavior would be expected from the large value of the energy defect for this excitation process. Since the quantity A
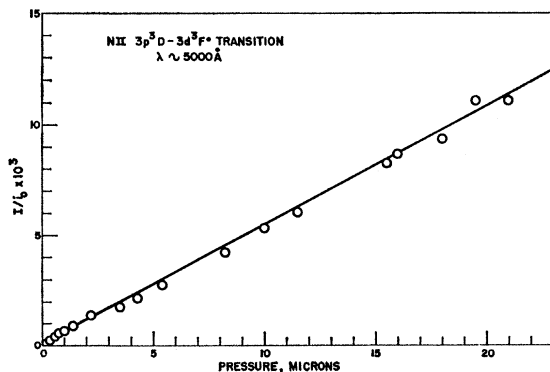
in this case is smaller relative to B than was the case for the first negative emissions, the data appear to have less scatter than in the latter case even though the determination of A is still as difficult.

The emission whose cross section has been measured here arises from the transition $3p\,^3D{-}3d\,^3F^0$. The upper $3d\,^3F^0$ state is presumably populated by ions which have cascaded down from a number of the highly excited NII states towards the $3s\,^3P^0$ state from which they can make a transition to the ground state. The experiments do not suggest, therefore, that there is any selective excitation of particular NII electronic states in the bombardment of N_2 by N_2^+.

NII Doppler Shift Experiment Results

Since the charge-exchange cross section for N^+ and N_2 is considerably smaller than for N_2^+ and N_2,[10] we
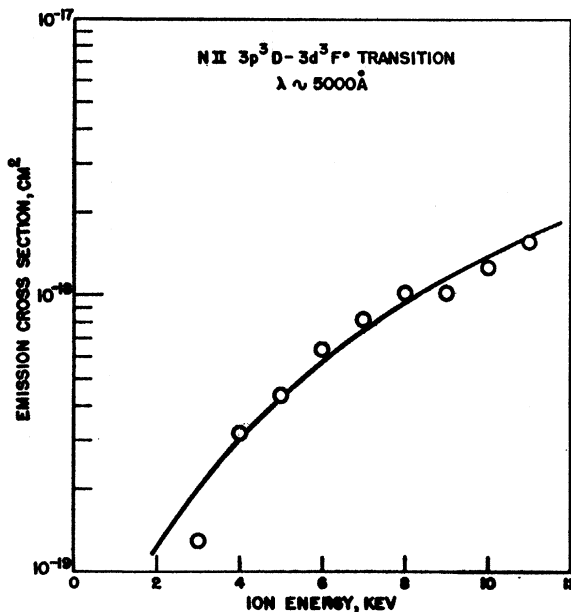
FIG. 9. Emission cross section versus ion energy for the NII $3p\,^3D{-}3d\,^3F^0$ ($\lambda{\sim}5000$ Å) lines.

can hope to see the Doppler-shifted NII emissions without the complication of charge exchange quenching.

This appears, in fact, to be the case. Figure 10 shows a high resolution spectrum of the $3s\,^1P^0{-}3p\,^1D$ ($\lambda3994$ Å) NII transition. Since this is a transition between singlet states, only one line is produced and it can be seen clearly with its Doppler-shifted component. All the NII transitions mentioned previously were examined for Doppler-shifted components and it was possible to identify a shifted line associated with each unshifted one. The shifted component was always at least as intense as the unshifted one.

These data, coupled with the fact that σ_{14} is relatively closer in value to σ_{13} than σ_4 to σ_2, suggest that the light

FIG. 8. Typical experimental I/i_0 versus pressure results for the NII $3p\,^3D{-}3d\,^3F^0$ ($\lambda{\sim}5000$ Å) lines.

observed arises from (13a), (13b), and (14) and that (13a) is slightly less probable than (13b). N^+ ions are apparently produced in excited states by ionizing collisions of primary beam ions and fast neutrals with the gas.

IV. CONCLUSIONS

The results of this research show that optical excitation processes can be successfully studied using an apparatus which integrates light produced along an extended path if the processes involved are simple enough that the mechanism can be firmly established. Since various parameters used in this experiment are derived from other experimental results, the absolute uncertainty which must be assigned to the emission cross sections is rather large. Stebbings, Turner, and Smith[10] assign an absolute uncertainty of $\pm 15\%$ to their values of σ_1 used here. Due to the agreement between investigators,[4,7] we can perhaps set the uncertainty in the electron N_2 excitation cross section which was used for calibration at $\pm 5\%$. Allowing $\pm 20\%$ uncertainty for such effects as possible loss of Doppler-shifted components of the emissions observed at high pressures we arrive at an absolute uncertainty of $\pm 40\%$ which seems reasonable.

The cross-section data show, as has been long observed qualitatively, that heavy ion excitation produces considerable population of higher molecular vibrational states. Rotational temperatures in excess of the gas temperature are apparently produced when the collision time is long enough for interaction with molecular rota-
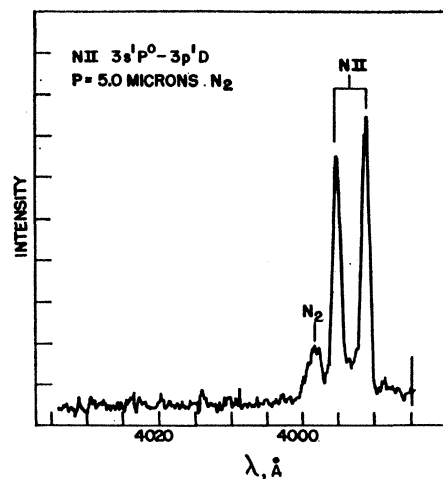

FIG. 10. Spectrum of N_{II} $3s$ $^1P^0-3p$ ^1D ($\lambda 3994$ Å) line excited by 10-keV N_2^+ on N_2 showing Doppler-shifted component.

tion. The results of the Doppler experiments are consistent with the mechanism proposed and, together with the cross section data, show that N_2^+ and N_{II} emissions are excited in different ways.

ACKNOWLEDGMENTS